COMPUTERS AND BIOMEDICAL RESEARCH 22, 136–159 (1989)

Stochastic Petri Net Modeling of Wave Sequences in Cardiac Arrhythmias

TOSHIO M. CHIN AND ALAN S. WILLSKY

Laboratory for Information and Decision Systems, Massachusetts Institute of Technology, Cambridge, Massachusetts 02139

Received November 23, 1987

We describe a methodology for modeling heart rhythms observed in electrocardiograms. In particular, we present a procedure to derive simple dynamic models that capture the cardiac mechanisms which control the particular timing sequences of *P* and *R* waves characteristic of different arrhythmias. By treating the cardiac electrophysiology at an aggregate level, simple network models of the wave generating system under a variety of diseased conditions can be developed. These network models are then systematically converted to stochastic Petri nets which offer a compact mathematical framework to express the dynamics and statistical variability of the wave generating mechanisms. Models of several arrhythmias are included in order to illustrate the methodology.

1. INTRODUCTION

Many cardiac arrhythmias can be diagnosed based solely on the timing of various types of waves observed in electrocardiograms (ECGs). To develop a classification algorithm for cardiac arrhythmias, these wave patterns must be represented in a mathematically formal way. The representation must be sophisticated enough to capture a wide variety of wave patterns, yet at the same time it must be simple enough to facilitate formulation of a classification algorithm. In this paper we describe a new methodology for the construction of concise models that accurately capture the wave timing characteristics of a wide variety of cardiac rhythms.

The motivation for our work comes from the successes and limitations of previous studies. In particular, in some previous studies, relatively simple Markov models have been used to describe patterns of particular observations of cardiac events. While other methods for arrhythmia classification exist (*11*, *12*), the use of such Markov models allows one to use powerful, *statistically optimal* classification algorithms. The major limitation is, however, that such models are appropriate only for a limited class of arrhythmias. For example, three-state Markov chains (*1*) and state-space formulations (*2*) have been used to model timing patterns for the most prominent ECG feature, the *R* wave, and successful classification algorithms have been developed based on them.

0010-4809/89 $3.00

Neither of these models, however, has been extended successfully to accommodate the timing of the *P* waves which are essential in the characterization of many cardiac arrhythmias (*10*).

These limitations of previous models provided the motivation for Doerschuk's work (*3*) on "interacting Markov chains" models. In this work Doerschuk has succeeded in developing statistical models that accurately capture the timing behavior of *P* and *R* waves together. His success can be attributed to the "physiological depth" of the models. Instead of modeling the wave pattern phenomena directly, he modeled the physiological events responsible for the generation of the ECG waves. The shortcoming of Doerschuk's models, however, is their comlexity due to the nature of the model representations used. In particular, the desire to use Markov chains forces one to deal simultaneously with fine-level timing parameters and more aggregate structural aspects of the model. Because of this, one loses some of the conciseness of description that one would like both for model construction and for any analysis or algorithm design based on these models.

In this paper we present a concise and flexible framework for modeling the electrical events characterizing various cardiac arrhythmias using stochastic Petri nets. In particular, in this setting we can quite easily separate and control the two significant aspects of cardiac activity highlighted in Doerschuk's model—namely the *timing* of events in different parts of the heart and the *interactions* among these parts. As we will see, the interactions specify the complete structure of the Petri net model, while timing information affects specific parameter values within the structure.

2. Aggregate Models of the Cardiac Conduction System

Since the two main functions of the cardiac electrical conduction system are generation and distribution of action potentials, the dynamics of the system can be described by a network of two types of elements. One of these is the *rhythm element*, which generates electrical signals, and the other is the *transmission element*, which distributes signals from one section of the system to another. The controlling mechanisms for macroscopic flows of electrical signals in the heart can be represented by a network of rhythm and transmission elements. In this section we introduce these elements and illustrate their use by representing the dynamics of several cardiac arrhythmias with such networks.

2.1. The Rhythm and Transmission Elements

We represent rhythm elements diagramatically as triangles and transmission elements as rectangles. The rhythm elements are used to describe the autorhythmic properties of cardiac muscle tissues; their primary function is periodic generation of electrical signals. Associated with a rhythm element are input and output terminals as well as several parametric variables that control the intervals of signal generation. The purposes of these terminals and parameters are as follows. (i) *Output*: The signal generated by the element is

sent to neighboring elements through the output terminal. (ii) *Input*. The autorhythmic cells can be stimulated by excitations in neighboring cells. The rhythm element receives such external stimulation through the input terminal. (iii) *Variables*. The fundamental parameter of a rhythm element is the *interval* at which it generates signals periodically. However, this basic interval can be altered especially when an external stimulation arrives through the input terminal. Thus, besides the basic interval, variables that quantitatively characterize the external influence on the function of the element are needed. Examples of such variables are the *absolute* and *relative refractory periods*, which play a major role in cardiac timing and phenomena such as resetting and inhibition.

The transmission elements are used to describe the delay of signals traveling through cardiac muscle tissues. A *bidirectional transmission element* has two pairs of input and output terminals. Signals can be transmitted through the element in either direction, but when two opposing signals meet in the element they annihilate each other. The variables associated with the transmission elements are the *transmission delays* for both directions, *refractory periods* which characterize the excitability of the two input terminals, and other parametric variables representing the factors that may influence the durations of transmission delays and/or refractory periods. A *unidirectional transmission element* is also represented by a rectangle but without the second pair of input and ouput terminals. Other variations of our basic elements, obtained by modifying the terminal behavior or internal variables of the elements, will be introduced in subsequent sections.

2.2. Signal Flow Block Diagrams

Rhythm and transmission elements allow us to model the timing of P and R waves and aberrancies of different rhythms at a relatively aggregate level. While it is certainly possible to use this modeling methodology to describe cardiac activity at a more detailed level (by partitioning the heart into a larger number of interacting rhythmic and conductive units, each representing a smaller portion of cardiac electrical pathways), the use to which we put this methodology here is at the other extreme. Specifically, by highlighting the mechanisms causing particular arrhythmias, we want to obtain the simplest possible models capturing characteristics of the corresponding P, R sequences. Such minimal representations should ultimately be of most value as the basis for the automated diagnosis of cardiac arrhythmias.

To illustrate this philosophy, consider the modeling of a perfectly normal heartbeat sequence. We can divide the cardiac conduction system into five stages based on their structural and functional differences—the SA node, intra-atrial conductive paths, AV node, Purkinje fiber conductive paths, and ventricles. Each tissue block can in fact excite autorhythmically, and all except the SA node and ventricles (which are the two ends of this electrical system) can conduct bidirectionally. As far as the modeling of a normal P, R sequence

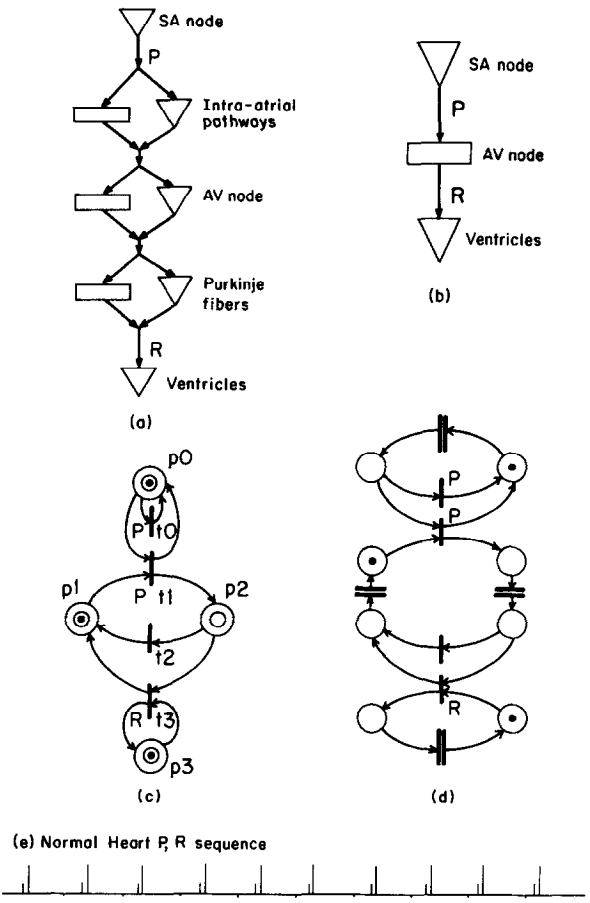

FIG. 1. Models of normal heart *P*, *R* sequences: (a) a physiologically motivated signal flow model, (b) a simplified signal flow model, (c) SPN implementation of (b) using the place-timed format, and (d) SPN implementation using the transition-timed format. A *P*, *R* sequence output of model (c) is shown in (e), in which the short and long lines represent *P* and *R* waves, respectively, and the ticks indicate 1-sec intervals. In (a) and (b), the triangles and rectangles represent rhythm and transmission elements, respectively (see Section 2.1). In the SPNs of (c) and (d), double circles and douoble bars, respectively, represent places and transitions with *nonzero* processing times.

is concerned, however, bidirectional conduction is an unnecessary detail since excitations conducting in the retrograde direction are never observed in such a sequence. Thus, a model constructed with unidirectional transmission elements instead of bidirectional elements is simpler yet phenomenologically just as accurate. Such a signal flow model is shown in Fig. 1a. The rhythm element representing the SA node does not have an input terminal because of the absence of retrograde-conducting excitation. The autorhythmic excitations of the SA node activate the atria and generate the *P* waves, indicated by the letter "P" in the figure. The excitation also bifurcates to activate the transmission element and reset the rhythm element of the intra-atrial pathways. The

excitation produced by the intra-atrial pathway is the result of either the transmission of the excitation originated in the SA node or its own autorhythmic activation. This is represented by the convergence of the outputs of the transmission and rhythm elements. The AV node and Purkinje fibers are represented by a parallel pair of transmission and rhythm elements, just like the intra-atrial pathways. The only differences among these three parts of the block diagram are the values of the parameters assigned to the respective transmission and rhythm elements (i.e., conduction delays, autorhythmic intervals, and absolute refractory periods). The output of the Purkinje fibers is directed to the ventricles whose activation produces the *R* wave, indicated by the letter "R" in the figure. This block diagram model implies that the autorhythmic period of the ventricles is larger than those of other parts of the heart so that the ventricles are "reset" frequently enough not to excite autorhythmically. In the model, therefore, the rhythm element representing the ventricles does not have an output terminal.

This model of the normal heart can be simplified further as follows: First, since in a normal cardiac sequence the autorhythmic rate in the SA node is the fastest and drives the entire system, the rhythm elements in the rest of the system are always "reset" before they can generate an autorhythmic excitation. We can, therefore, delete the three rhythm elements used to model the autorhythmicity of the intra-atrial pathways, AV node, and Purkinje fibers. After these rhythm elements are removed, the remaining stages that separate the two wave generators collectively form a series of three transmission elements. These transmission elements can be combined into one aggregate element, which we call the "AV node" for simplicity. The simplified model of the normal heart is shown in Fig. 1b.

2.3. Modeling of Common Arrhythmic P, R Wave Sequences

In this subsection, we represent the dynamics of several cardiac arrhythmias using block diagrams consisting of rhythm and transmission elements. Figures 2a to 6a show such models for several examples, and Figs. 2b to 6b present the *P*, *R* wave sequences obtained from simulations of the models (see Section 4 for details of the simulations). *P* waves are represented by short vertical lines, *R* waves by longer lines, and morphologically abnormal waves by lines with small squares at their tips. The interval of time ticks is 1 sec.

1. Extrasystole—ectopic beat. (*i*) *Phenomenology.* In this condition, non-SA nodal tissue becomes, either continuously or sporadically, a pacemaker for the heart. The waves initiated by such ectopic rhythm sources are *atrial premature beats* (APB) or *ventricular premature beats* (VPB). In case of VPB, *retrograde P waves* may be observed as well. The normal rhythm source at the SA node can be reset or inhibited by retrograde excitations.

(*ii*) *Modeling.* Ectopic beats are caused by abnormally fast autorhythmic rates at non-SA nodal tissues. Rhythm elements are used to represent such ectopic sources.

(*iii*) *Examples.* Figures 2a and 3a show examples of block diagrams of APB and VPB, respectively. Both models consist of three stages—the atria, AV nodes, and ventricles. In the APB model (Fig. 2a) the atrial stage has two rhythm elements, one for the normal SA nodal beats and the other for the atrial ectopic beats. The output of each rhythm element resets the other rhythm element and activates the transmission element representing the AV node. The rest of the model is identical to the normal heart described before (Fig. 1b). The *P* waves produced by atrial ectopic beats usually have abnormal shapes; in the model "$\bar{P}$" indicates that the output of the rhythm element representing the ectopic source generates such abnormal *P* waves. In the VPB model (Fig. 3a) the ectopic source is generally thought to be in the ventricular tissue. Thus, the rhythm element representing the ventricles has an output terminal whose activation produces a premature, abnormally shaped *R* wave (denoted by "$\bar{R}$" in the figure). Since the excitation generated by the ventricles conducts in the retrograde direction toward the atria, a bidirectional transmission element is used to represent the AV node. Retrograde activation of the atria causes a retrograde *P* wave ("$\bar{P}$") and rests the SA nodal autorhythmic source.

2. *Extrasystole—coupled beat.* (*i*) *Phenomenology.* This category deals with premature waves whose timings display strong correlation with the timings of normal waves. Specifically, these premature waves are synchronized with the normal beats, and the intervals between premature waves and preceding normal waves are fairly constant and are called the *coupling intervals.*

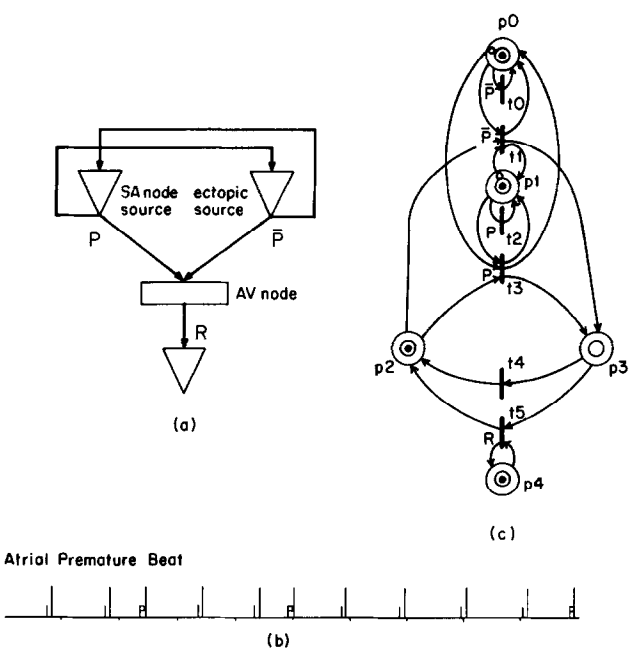

FIG. 2. Atrial premature beat: signal flow model (a) and an example of *P*, *R* sequence (b) obtained by the simulation of the SPN implementation (c) of the model.

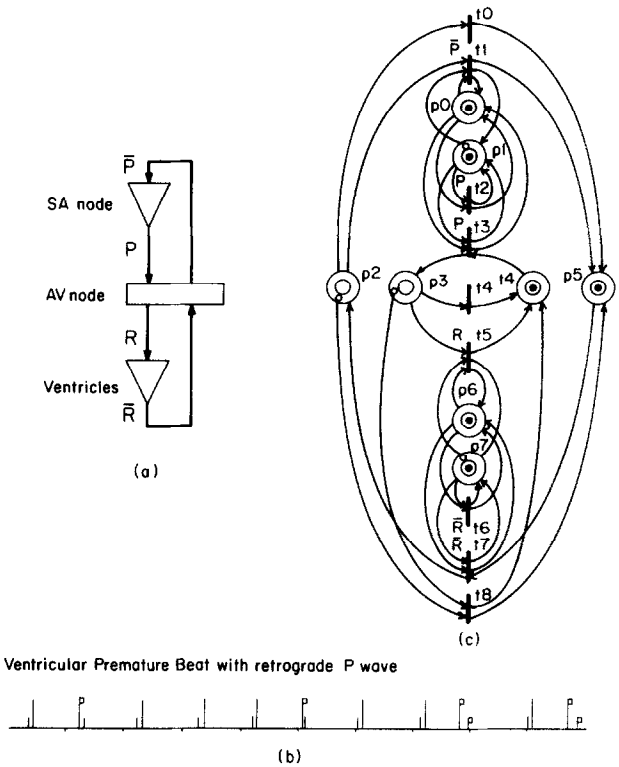

FIG. 3. Ventricular premature beat: signal flow model (a) and an example of P, R sequence (b) obtained by the simulation of the SPN implementation (c) of the model.

(*ii*) *Modeling*. Although there are several physiological explanations for the origin of the coupling intervals, a convenient way to describe the phenomenon is to use a hypothetical electrical conduction channel, called the *reentrant pathway*, residing within the muscular wall of a heart chamber and having a conduction delay whose value is equal to the coupling interval. It receives an excitation when the chamber is excited to contract, delays the excitation for the amount of the time specified by its conduction delay parameter, and then returns the excitation back to the chamber. This leads to a *second*, abnormal contraction of the chamber (and generation of an associated ECG wave) following the normal contraction arising from the direct pathway. In the block diagram, the reentrant pathway is represented by a unidirectional transmission element.

(*iii*) *Example*. Figure 4a shows the block diagram for *bigeminy*. The first two stages of the model—the SA and AV nodes—are the same as the normal heart. The output of the AV node activates both the ventricles (producing the normal R wave) and the reentrant pathway. The reentrant pathway delays the excitation and activates the ventricles (producing the abnormal R wave). The coupling interval is modeled by the delay parameter of the transmission

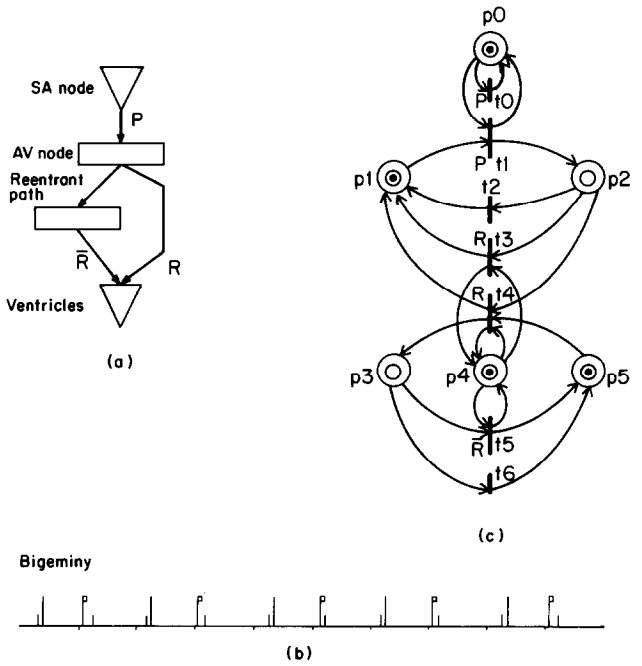

FIG. 4. Bigeminy: signal flow model (a) and an example of *P*, *R* sequence (b) obtained by the simulation of the SPN implementation (c) of the model.

element representing the reentrant pathway. The normal conduction wave (initiated by the SA node) immediately following the premature *R* wave arrives at the ventricle during its absolute refractory period. Thus, the normal excitation is blocked, and the corresponding *R* wave is not produced. This is observed as the relatively long interval between a premature *R* wave and the succeeding normal *R* wave (Fig. 4b).

3. AV conduction block. (i) Phenomenology. This category includes arrhythmias caused by abnormalities in conduction between the atria and the ventricles. In a *third degree AV block*, the AV node is effectively unable to conduct excitations. Thus, the contractions of the ventricles must be paced by the autorhythmicity of the AV node, Purkinje fibers, or ventricular musculature itself. The resulting *P*, *R* wave sequence displays a case of *AV dissociation*, a phenomenon in which the rhythm of the *R* waves is independent from that of the *P* waves. In *second degree AV block*, not all the atrial excitations are blocked by the AV node. For example, when only two out of three *P* waves are followed by *R* waves, the condition is referred to as 3:2 block. In a *Wenckebach block*, the SA node generates excitations at a constant rate, but the *P–R* interval grows progressively longer during several beats until there is a *P* wave not followed by an *R* wave. The next *P* wave is followed by an *R* wave with a normal, short *P–R* interval; then, the interval again grows progressively longer over the next several beats as the pattern is repeated. Figure 6b shows an

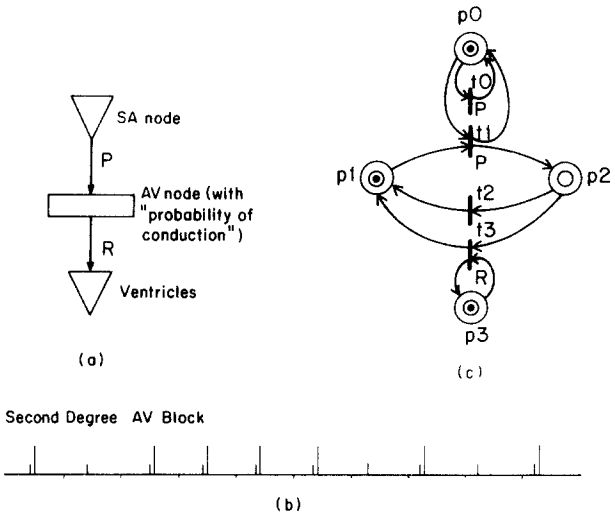

FIG. 5. Second degree AV block: signal flow model (a) and an example of P, R sequence (b) obtained by the simulation of the SPN implementation (c) of the model.

example of a P, R sequence displaying a Wenckebach block. Finally, in *first degree AV block*, no R wave is missed after any P wave, but the P–R interval is abnormally prolonged.

(*ii*) *Modeling*. AV conduction blocks are caused by various disease conditions inside the AV node. Consequently the models of these rhythms are obtained by modifying (or in the case of third degree AV block, by eliminating) the transmission element representing the AV node in the normal heart model.

(*iii*) *Examples*. Figure 5a shows a model of second degree AV block. Note that the transmission element has an extra parameter called "probability of conduction." In 3:2 block, for example, this probability is set to 2/3. Figure 6a shows a model for the Wenckebach phenomenon. A completely different transmission element must be used to describe the dynamics of the AV node. In Wenckebach, events in the current beat are dependent on the events in the previous beats. For example, every P–R interval must be longer than the previous interval unless the R wave is missing from the previous beat; if the R wave is missed the P–R interval must become short again. The transmission element, therefore, must have a "memory" of its action in the previous beats to determine how it behaves in the current beat. This requires us to describe the transmission element itself as a dynamic system. Detailed specification of the behavior of such a transmission element is discussed in Section 4.

In the preceding description of the cardiac electrical conduction system, we have identified several of its dynamic properties which enable us to characterize the P, R wave sequences of the cardiac arrhythmias. Two important features of the signal flow block diagrams for cardiac arrhythmias should be noted: One is that the system dynamics are regulated by local timing parameters (e.g., autorhythmic periods, conduction delays, and refractory periods),

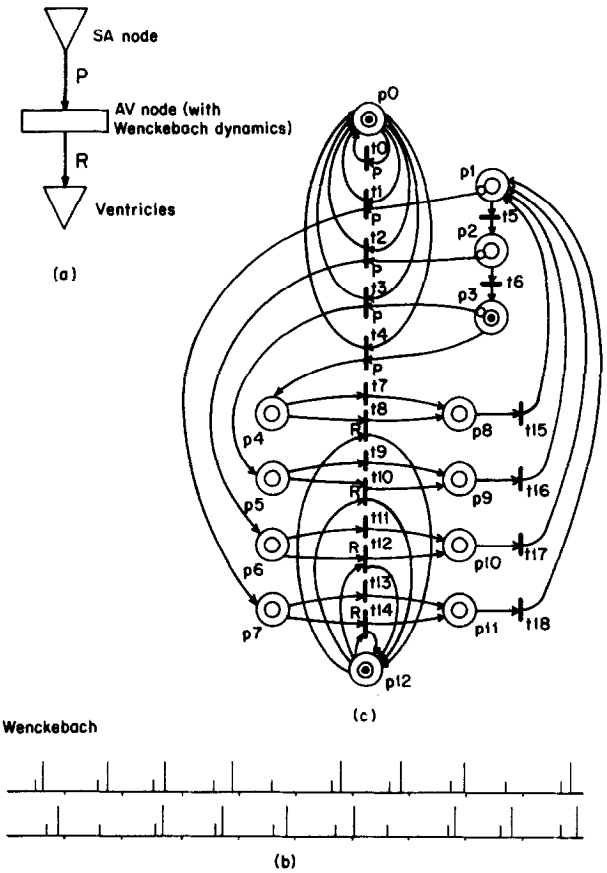

FIG. 6. Wenckebach phenomenon: signal flow model (a) and an example of P, R sequence (b) obtained by the simulation of the SPN implementation (c) of the model.

and the other is the concurrency of the dynamics (e.g., the SA node is in its refractory period while the AV node is conducting excitation). In other words, using the block diagrams introduced in this section we have characterized the mechanisms of various cardiac arrhythmias as *concurrent timing processes*. Stochastic Petri nets represent a modeling framework developed explicitly to capture dynamics of this type and therefore represent an ideal choice for the precise mathematical implementation of the dynamics captured in our signal flow models. This is the subject of the next two sections.

3. STOCHASTIC PETRI NETS

As indicated in the previous section, the nature of cardiac behavior makes stochastic Petri nets a natural choice for modeling of cardiac rhythms. In this section we review the basic features of elementary stochastic Petri nets.

3.1. Petri Nets

Petri nets (*4, 5*) are abstract models of information flow, and they are particularly useful in describing and analyzing the flow of information and control in systems which exhibit asynchronous and concurrent activities.

Structure. Petri nets are commonly represented pictorially as directed graphs. Figure 7 shows an example of a Petri net. There are four structual components—two types of nodes, called *places* and *transitions*, and two types of directed arcs, *input* and *output arcs*. A place is represented by a circle ("p0" to "p6" in Fig. 7) and a transition by a bar ("t0" to "t5"). All the directed arcs in a Petri net connect a node of one type with a node of the other type.

Dynamics. The dynamics of Petri nets are represented by the positions and movements of markers called *tokens*. Tokens are pictorially represented by dots inside places. In the example (Fig. 7), each of the places p0, p2, and p6 has a single token. Tokens can be moved to other places along directed arcs by *firing* transitions on the arcs. A transition can fire only if it is *enabled*, i.e., if *all* its input arcs are connected to places possessing tokens. In the example, t1 and t2 are enabled, and t3 is not enabled because p3 does not have a token.

Decision rules. Note that in the preceding example t1 and t2 cannot fire at the same time because firing one of them takes the token out of p0 and disables the other. Those transitions competing for the same token(s) are described to be "in conflict," or "to form a *conflict set*" (*7–9*). Thus, without the specification of some type of *decision rule* for the resolution of all such potential conflicts, the dynamics of the net would not be well-defined. A variety of decision rules are possible—for example, preferential (e.g., the firing of t2 takes procedence over the firing of t1) and probabilistic (t2 fires with probability 0.7 and t1 with probability 0.3)—and these can be chosen to model different phenomena.

3.2. Stochastic Petri Nets

The original Petri nets, as described above, are defined without the notion of time; however, in *timed Petri nets* some explicitly defined timing parameters ("processing times") influence the evolution of the state of the nets. *Stochastic Petri nets* (SPNs) are those timed Petri nets in which the processing times are specified probabilistically. There are two basic ways in which processing times are introduced into Petri nets (see Ref. (*6*) for more on this and related issues). In a *transition-timed* SPN, the processing time is associated with transitions.

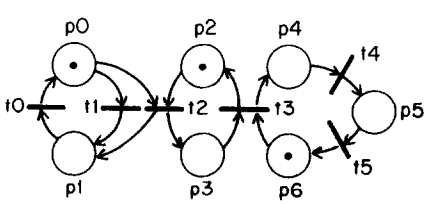

FIG. 7. An example of Petri net.

When a transition is enabled, a sample of the random variable representing the corresponding processing time is chosen, and the transition must wait for this amount of time before it can fire. Note that in this setting an enabled transition waiting to fire can become disabled by the firing of other transitions (i.e., those "in conflict" with it). This allows us to model *interruption* which is important in cardiac modeling—e.g., we need to be able to model the interruption of the cycle of an autorhythmic unit due to excitation from other elements of the cardiac model.

An alternative class of SPNs consists of *place-timed* SPNs in which the processing times are associated with places. When a token enters a place, it initially becomes "unavailable" to the rest of the system until the corresponding probabilistically chosen processing time elapses. A transition is not enabled unless all its input arcs are connected to places with "available" tokens. An enabled transition fires immediately (subject to, of course, the outcome of any associated decision rule).

A critical limitation of classical place-timed SPNs is that they model a strictly smaller class of phenomena than transition-timed SPNs, and in particular they cannot capture the interruption process referred to previously. On the other hand, place-timed SPNs offer a much more concise graphical description of cardiac behavior. For example, compare the normal heart models in Figs. 1c and 1d using the two SPN formats. In Fig. 1c double circles are used to represent places with nonzero processing time, while in Fig. 1d double bars represent transitions with nonzero processing times.

As we will see in the next section, some relatively simple models of cardiac arrhythmia can have complex topologies. Graphical conciseness is, therefore, quite desirable as it facilitates not only interpretation of the models but also representation of more complex physiological mechanisms. Therefore, in order to allow us to use the simpler place-timed SPN representation we augment it with one additional feature that allows it to represent just as rich a range of behaviors as transition-timed SPNs. Specifically, we introduce the notion of an *interruptable processing time*. A place with an interruptable processing time has a special output arc through which a token inside it is always "available" to the rest of the system. For example, place p1 in Fig. 2c has a special output arc, marked by a small circle, through which the token inside it is always available to the rest of the system. Thus, while the transition t2 cannot fire until the processing time at the place elapses, t1 can fire as soon as it is enabled. Firing of t1, therefore, may "interrupt" the processing time assigned to the place.

4. SPN Models of Cardiac Arrhythmias

In Section 2 we modeled several common cardiac arrhythmias with networks of rhythm and transmission elements. In this section we implement various rhythm and transmission elements with SPNs. We then discuss briefly how to connect these SPN elements to form SPN cardiac arrhythmia models followed

by a presentation of several examples of such SPN models of cardiac arrhythmias.

4.1. Fundamental Building Blocks

Recall from Section 2 that variations in autorhythmic rates, conduction delays, and refractory periods characterize functions of individual rhythm and transmission elements which are in turn responsible for most cardiac arrhythmias. We now present SPN implementations of subelements ("units") controlling these timing quantities.

(1) Autorhythmic unit. Figure 8a shows the basic SPN building block for an autorhythmic unit. The period of the rhythm is represented by the processing time associated with the single place p0. The transition t1 represents the output of the autorhythmic unit. The incomplete arcs to and from t1 are parts of the SPN fragment representing the neighboring tissue which receives excitation from the autorhythmic unit. The reception of excitation is accomplished by firing of t1. As soon as the token becomes available in p0, it is fired back into p0 via either t0 or t1 to recycle the process. An autorhythmic activity may or may not induce activity in the neighboring tissue depending on whether the tissue is in refractory period or not. But if the tissue is ready to be excited, the activity is always transferred to it. Thus, the decision rule for the conflict set {t0, t1} is assigned so that is chooses t1 preferentially over t0.

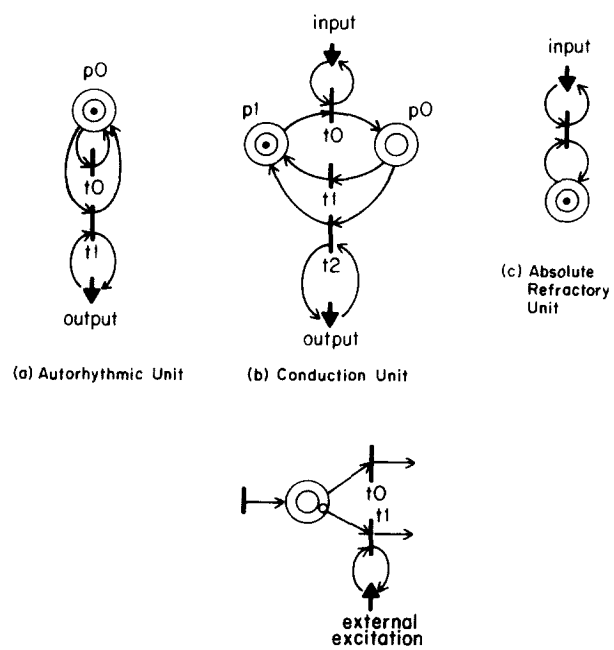

FIG. 8. Fundamental units for SPN implementation of signal flow models.

(2) *Conduction units.* A conduction unit receives excitation from one tissue (the input tissue), holds the excitation for a certain amount of time (the conduction delay), and transfers the excitation to another tissue (the output tissue). The conduction delay of such a unit is specified by an accompanying probability density functions. Figure 8b shows the SPN implementation of the basic conduction unit. If the token in the place p1 is "available" (meaning that the conduction tissue has come out of the refractory period and is excitable), the transition t0 fires when it receives excitation from the input tissue. The token then enters the place p0 whose processing time represents the conduction delay. After the delay, the token is fired back into p1 by t1 or t2. When the token is in p0, t1 is always enabled while t2 is enabled only when the output tissue is ready to receive the excitation. Since excitation is always transferred to output tissue not in its refractory period, the decision rule is assigned so that t2 is preferentially chosen over t1 whenever they are in conflict. The processing time associated with p1 represents the time required for the conduction unit to become ready to receive a new excitation after it has processed a preceding excitation; thus, this processing time can be considered a collective absolute refractory period for all the cells in the conduction tissue. The roles of relative refractory periods in conduction of excitations are discussed later.

(3) *Refractory periods.* There are two kinds of refractory periods—absolute and relative. When the tissue is in an absolute refractory period, an oncoming excitation is blocked. On the other hand, when the tissue is in a relative refractory period, an oncoming excitation induces the tissue to be activated with abnormal characteristics such as elongated conduction delay (e.g., Wenckebach). Figure 8c shows a basic absolute refractory unit. The processing time assigned to the single place is the absolute refractory period, and the transition cannot fire unless the token in the place becomes available. Figure 8d shows a relative refractory unit, using a place with an interruptable processing time. The processing time associated with the place represents the relative refractory period. The firing of t0 represents the normal course of action where the tissue becomes completely ready to receive a new excitation. On the other hand, the firing of t1 represents a premature activation of the tissue by an external excitation, and the tissue is expected to respond abnormally.

4.2. SPN Model of the Normal Heart

In Section 2 we showed that the normal heart could be modeled with three elements representing the SA node, AV node, and ventricles (Fig. 1b), and these elements can, respectively, be implemented as the autorhythmic unit, conduction unit, and absolute refractory unit described above. The resulting SPN model is shown in Fig. 1c. The output of the model is the timing of generation of P and R waves, and these are represented by firing of the transitions t0, t1, and t3, i.e., t0 and t1 for P wave and t3 for R wave. The parameters of the model are the processing times associated with the places, p0, p1, p2, and p3, and these correspond with the autorhythmic interval of the

SA node, the refractory period of the AV node, conduction delay of the AV node, and the refractory period of the ventricles, respectively. Figure 1e shows the output of a simulation run of this SPN model (with short and long vertical lines representing P waves and R waves, respectively, and tick marks measuring 1-sec intervals.) The processing times used in the simulation run are listed in Table 1.

The simplicity of the models in Fig. 1 has come about because unnecessary details are deliberately left out. For example, in the signal flow model (Fig. 1b),

TABLE 1

MODEL PARAMETERS

Normal heart (Fig. 1c)	
p0 (SA rhythm)	{0.92, 0.96, 1.00, 1.04, 1.08}
p1 (AV refractory period)	{0.3}
p2 (AV conduction delay)	{0.08, 0.10}
p3 (Vent. refractory period)	{0.3}
Atrial premature beat (Fig. 2c)	
p0 (ectopic rhythm)	{0.6, 0.8, 1.5}*
*Nonuniform distribution: Prob(0.6) = Prob(0.8) = 0.15; Prob(1.5) = 0.70	
p1 (SA rhythm)	{0.92, 0.96, 1.00, 1.04, 1.08}
p2 (AV refractory period)	{0.3}
p3 (AV conduction delay)	{0.08, 0.10}
p4 (Vent. refractory period)	{0.3}
Ventricular premature beat (Fig. 3c)	
p0 (SA refractory period)	{0.3}
p1 (SA rhythm)	{0.92, 0.96, 1.00, 1.04, 1.08}
p2 (retrograde conduction delay)	{0.14, 0.16}
p3 (AV conduction delay)	{0.08, 0.10}
p4 (AV refractory—normal)	{0.3}
p5 (AV refractory–retrograde)	{0.3}
p6 (ventricles refractory)	{0.3}
p7 (ectopic rhythm)	{0.6, 0.8, 1.5}*
*Nonuniform distribution: Prob(0.6) = Prob(0.8) = 0.15; Prob(1.5) = 0.70	
Bigeminy (Fig. 4c)	
p0 (SA rhythm)	{0.92, 0.96, 1.00, 1.04, 1.08}
p1 (AV refractory period)	{0.3}
p2 (AV conduction delay)	{0.08, 0.10}
p3 (reentrant conduction delay)	{0.7, 0.8}
p4 (Vent. refractory period)	{0.5}
p5 (reentrant refractory period)	{0}
Second degree AV block (Fig. 5c)	
p0 (SA rhythm)	{0.92, 0.96, 1.00, 1.04, 1.08}
p1 (AV refractory period)	{0.3}
p2 (AV conduction delay)	{0.08, 0.10}
p3 (Vent. refractory period)	{0.3}
Decision rule for {t0, t1} Prob(t0) = 0.25; Prob(t1) = 0.75	

TABLE 1—*Continued*

Wenckebach (Fig. 6c)	
p0 (SA rhythm)	{0.92, 0.96, 1.00, 1.04, 1.08}
p1 (AV relative ref. subperiod)	{0.16}
p2 (AV relative ref. subperiod)	{0.16}
p3 (AV relative ref. subperiod)	{0.16}
p4 (AV conduction delay)	{0.16, 0.20}
p5 (AV conduction delay)	{0.20, 0.24}
p6 (AV conduction delay)	{0.24, 0.28}
p7 (AV conduction delay)	{0.28, 0.32}
p8 (AV absolute refractory)	{0.48}
p9 (AV absolute refractory)	{0.56}
p10 (AV absolute refractory)	{0.68}
p11 (AV absolute refractory)	{0.80}
p12 (Vent, absolute refractory)	{0.28, 0.32, 0.36}

Note. The processing times and probabilistic decision rules for the models in Figs. 1 to 6 are shown. The processing times take the discrete values listed here. They are uniformly distributed among the indicated set of values unless noted otherwise. The unit of time is the *second.*

a unidirectional transmission element rather than a more complex bidirectional transmission element was used to represent the AV node because it is known that no retrograde conduction is obesrved in a normal *P, R* wave sequence. The rhythm element representing the SA node does not need an input terminal also because of the absence of retrograde conduction. The normal heart is, of course, capable of conducting retrograde excitations, but modeling at such level of accuracy is not necessary to capture the behavior of a normal *P, R* wave sequence.

4.3. Rhythm and Transmission Elements

Rhythm elements. The most simple rhythm elements are the pacemaker (Fig. 9a) and terminal (Fig. 9f). An example of a pacemaker is the SA node in the normal heart; the sole function of the element is to generate excitation periodically. The single parameter for the pacemaker is the period of the autorhythmic excitation, and this is represented by the processing time at the place. An example of a terminal is the ventricle in the normal heart; the element simply receives and absorbs incoming excitations. The single parameter of the terminal is the absolute refractory period. If the terminal depicted in Fig. 9f represents the ventricle, firing of the transition represents the generation of the *R* wave.

In reality, pacemaker tissues can receive excitation (for example, the SA node can receive retrograde-conducting excitation) and can be reset or inhibited. A more accurate model of pacemakers should have such dynamic properties. Moreover, a way to make the model more accurate than this is to include an absolute refractory period during which the pacemaker tissue cannot

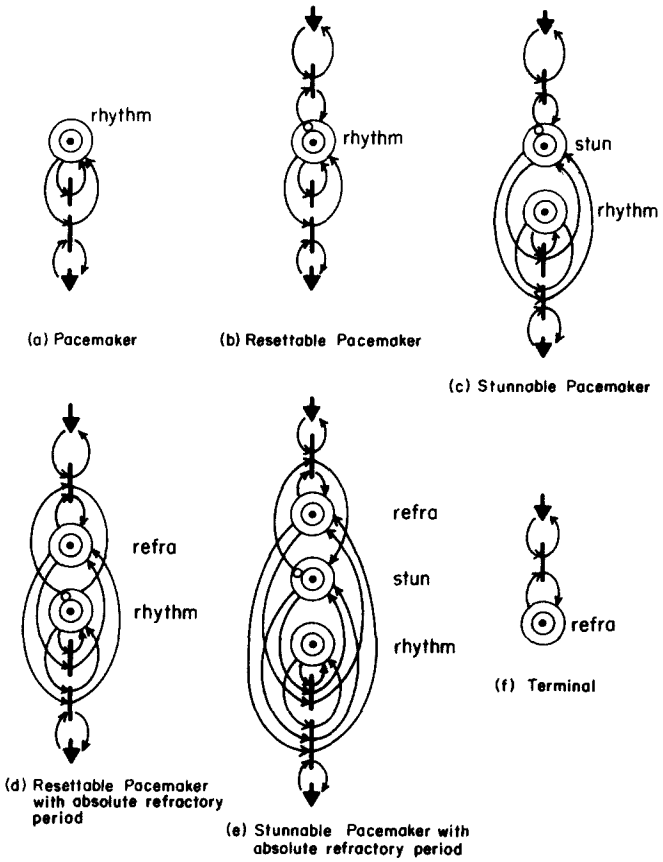

FIG. 9. SPN implementations of common rhythm elements. The processing time assigned to a place is period of autorhythmicity (denoted as "rhythm" in the figure), absolute refractory period ("refra"), or duration of inhibition ("stun").

be reset or inhibited. These functional variations of the rhythm element can be used in arrhythmia modeling, and corresponding SPN building blocks are presented in Fig. 9.

Transmission elements. The most simple transmission element is the unidirectional element depicted in Fig. 10a and employed in the construction of the normal heart model. One functional variation is the transmission element with a probability of conduction, shown in Fig. 10b, which is necessary in the modeling of second degree AV block. An extra transition t0 has been added. The transitions t0 and t1 are in conflict; firing of t0 does not activate the transmission element while firing of t1 does. The decision rule for the conflict set {t0, t1} is a probabilistic policy where the probability "q" of choosing t1 is equal to the probability of the conduction.

Another functional variation is the bidirectional transmission element. It is more realistic than the unidirectional element, while its implementation is

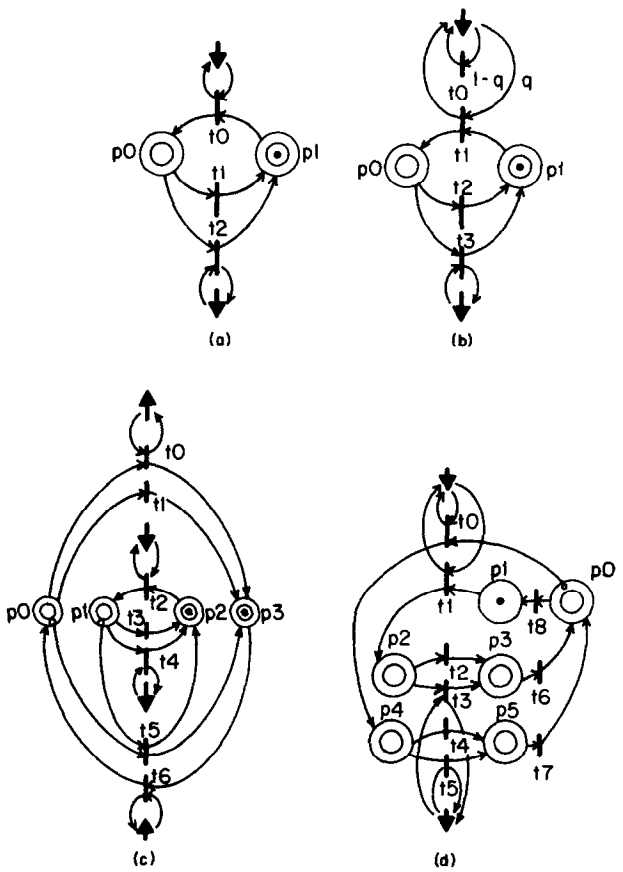

FIG. 10. SPN implementation of common transmission elements: (a) basic unidirectional, (b) unidirectional with probability of conduction "q," (c) bidirectional, and (d) unidirectional with variable timing characteristics.

slightly more complex than a simple combination of two unidirectional elements. The complexity is due to the necessity of modeling annihilation of two excitations colliding inside the element. Figure 10c shows the bidirectional transmission element. It is basically two undirectional elements superimposed, with the addition of the transition t5 and the use of interruptable processing times at p0 and p1. When excitations collide in the element, t5 fires, and no activity reaches the outputs.

Another variation can be seen in the transmission elements capable of generating the Wenckebach phenomenon. The lengths of the conduction delay and refractory period of such a transmission element are determined by its interaction with neighboring elements. Figure 10d shows an SPN implementation of such a transmission element. The relative refractory period is represented by the interruptable processing time of p0. The normal course of token movement is p0–p1–p2–p3–p0. However, when the element is excited during

its relative refractory period, the token travels the abnormal course p0–p4–p5–p0. The conduction delays through the element are represented by p2 and p4, while the absolute refractory periods are represented by p3 and p5. For the Wenckebach phenomenon, the processing time for p4 should be set longer than that for p2 while that for p3 should be longer than that for p5. We have mentioned in Section 2 that this element should have "memory." The element in this example registers whether the previous excitation has arrived during its relative refractory period or not by the location of the token, i.e., whether the token is in the abnormal loop or the normal loop. Note that the token takes a longer time to go through the abnormal loop so that the chance of receiving the next external excitation while it is in absolute or relative refractory period is greater. To model common Wenckebach blocks, more than one abnormal loop may be necessary. Such a Wenckebach model is presented in Subsection 4.5.

Several functional variations of the transmission element have been discussed here. Although their coverage is not exhaustive, most common cardiac arrhythmias can be modeled using the variations of the elements discussed above. The SPN implementations of these are presented in Fig. 10.

4.4. Interfacing the Elements

Case I: connecting a single output to multiple inputs. Figure 11a shows a rhythm element sending excitation to two transmission elements. When the rhythm element sends an excitation, each of the two transmission elements can be in two states—ready to receive the excitation or not ready to receive. Thus, the number of states of the receivers is four ($= 2^2$), and four transitions are used

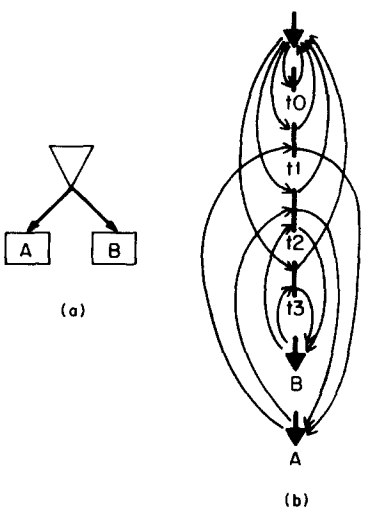

FIG. 11. An example of interfacing SPN blocks—fan-out: (a) The rhythm element sends its output to two transmission elements. (b) The SPN implementation of interface of the three elements in (a).

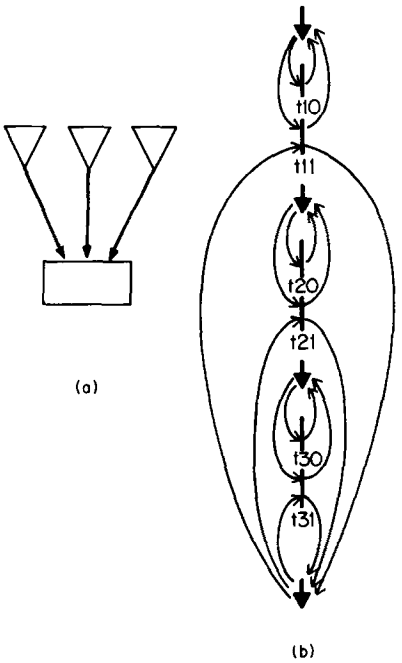

FIG. 12. An example of interfacing SPN blocks—fan-in: (a) Each of the three rhythm elements can activate the transmission element. (b) The SPN implementation of interface of the four elements in (a).

to implement this interface (Fig. 11b). Each of the four transitions represent the following cases:

t0—neither of the transmission elements is ready to receive.
t1—element A is ready to receive, but not element B.
t2—both elements are ready to receive.
t3—element B is ready to receive, but not element A.

In general, when a single output is trying to distribute an excitation to N inputs, 2^N transitions are required.

Case II: connecting multiple outputs to a single input. Figure 12a shows three rhythm elements sending excitation to a transmission element. Since each sender may or may not be able to excite the receiver, six ($= 2 \times 3$) transitions are needed (Fig. 12b). In general, when N outputs are trying to access to a single input, $2N$ transitions are required.

4.5. SPN Models of Cardiac Arrhythmias

SPN implementations of the cardiac arrhythmias discussed in Section 2 are presented in Figs. 2c to 6c. The results of simulation based on these SPNs are presented in Figs. 2b to 6b. The values of the model parameters used in the simulation runs are listed in Table 1.

Atrial premature beat (*Fig. 2c*). The block diagram model of Fig. 2a is implemented with an SPN. Two "resettable pacemakers" are used to represent the normal (SA nodal) and ectopic rhythm sources in the atria. Firing of one source resets the other source; thus, after every beat the two sources race to initiate the next excitation. The processing times at p0 and p1 correspond with the autorhythmic intervals of the ectopic and normal sources, respectively. The probability density function of the processing time at p0 has a broader distribution than the one at p1, so that with a certain probability the ectopic source can generate excitation at a noticeably shorter interval than the normal source. The firing of t0 or t1 represents an excitation of the ectopic source, and it produces a P wave with an abnormal morphology, denoted by "$\bar{P}$." The firing of t2 or t3 represents an SA nodal excitation producing a normal P wave. The rest of the model is similar to the normal heart model. The places p3 and p2 represent the AV nodal conduction delay and its refractory period, respectively, and they are parts of the "basic unidirectional transmission element." The ventricles are modeled by the "terminal" element (p4 and t5). Firing of t5 produces an R wave. In the simulation result (Fig. 2b), the short verticle lines with small squares at their tips represent P waves initiated by the ectopic source.

Ventricular premature beat (*Fig. 3c*). This model, whose block diagram was introduced in Fig. 3a, consists of two "resettable pacemakers with refractory periods" and a single "bidirectional transmission element." The places p1 and p0 are the autorhythmic interval and absolute refractory period at the SA node, respectively, while p7 and p6, respectively, are those at the ventricles. The conduction delay and absolute refractory period at the AV node are represented by p3 and p4, respectively, for the antegrade (normal) direction and by p2 and p5, respectively, for the retrograde direction. Correspondence between firing of the transitions and production of the waves is as follows: t2 and t3 for normal P, t5 for normal R, t6 and t7 for ectopic (premature) R, and t1 for retrograde P. In the simulation result (Fig. 3b), the R waves and P waves with a small square on the tips denote the ectopic R waves and retrograde P waves, respectively. Observe that a pairing of a normal P wave and an ectopic R wave occurring at about the same time is followed by neither a normal R wave nor a retrograde P wave. Nearly simultaneous autorhythmic excitations at the two rhythm sources of the model produce a normal P and ectopic R waves, but the resulting flows of excitations have collided inside the transmission element and blocked each other.

Bigeminy (*Fig. 4c*). As described in Section 2, we use the concept of "reentrant pathway" to explain the mechanism of bigeminy. The model is almost the same as the normal heart model. The only difference is the presence of the reentrant pathway represented by the basic unidirectional transmission element consisting of p3 and p5.

Second degree AV block (*Fig. 5c*). The topology of this model is exactly the same as that of the normal heart, but in this model the decision rule for the conflict set {t0, t1} is no longer deterministic. Whenever a conflict exists, t1 is

chosen over t0 with a probability equal to the probability of conduction. Figure 5b is the result of simulation of a "4:3 block," where the probability of conduction is 3/4. Since in this model conduction blocks are independent events, they can occur in consecutive beats. In reality, however, such consecutive blocks are rare. Making sure that conduction blocks are isolated can be accomplished at the expense of a more complex model. Specifically, decision by the model to cause a block in a particular beat must be influenced by whether or not a block has occurred in the previous beat; i.e., the model must have "memory." The model of the Wenckebach phenomenon described next illustrates the implementation of a memory feature of this type.

Wenckebach (Fig. 6c). The block diagram of this Wenckebach model consists of two rhythm elements and a transmission element (Fig. 6a). Two "basic rhythm elements" are used to represent the SA node (p0) and ventricles (p12). The single transmission element is a "stunnable transmission element" similar to that described in Subsection 4.3 and Fig. 10d, but this element has two extra "abnormal loops." The loops, in the order of increasing transit times, are (i) p1–p2–p3–p4–p8, which is the normal loop; (ii) p1–p2–p3–p5–p9; (iii) p1–p2–p6–p10; and (iv) p1–p7–p11. The processing times at p4, p5, p6, and p7 (in the order of increasing length) represent the AV conduction delays (thus the *P*, *R* intervals). Those at p8, p9, p10, and p11 are the absolute refractory periods of the AV node. The relative refractory period is divided into three subperiods of equal lengths—early (p1), middle (p2), and late (p3). Each of these subperiods is assigned an interruptable processing time. An interrupt occurs when the SA node (p0) excites while the token of the AV node is in one of these relative refractory subperiods, initiating an entry into the corresponding abnormal loop. *P* waves are produced by the firing of t0, t1, t2, t3, or t4, while *R* waves, by the firing of t8, t10, t12, or t14. The simulation result (Fig. 6b) clearly displays the Wenckebach phenomenon.

This section along with Section 2 has illustrated a systematic way in which we can derive SPNs for cardiac arrhythmia models. Specifically, the physiological mechanism of an arrhythmia is first described as a signal flow block diagram with rhythm and transmission elements. The block diagram may be simplified greatly by removing details unnecessary to characterize the *P*, *R* sequence of the particular arrhythmia under study. Such a high level description can then be translated into an SPN in an element-by-element fashion using the implementations presented in this section (and straightforward extensions of them if needed). Thus, we have a method to derive the SPN structure (topology), initial token placement, and decision rules. The last piece of information required to complete the model is the parameters, i.e., probability distributions for the processing times and probabilistic decision rules. We emphasize that two sets of parameters assigned to the same SPN structure can lead to two outputs drastically different from each other. For example, the SPN structure for bigeminy (Fig. 4c) can be programmed to output a *P*, *R* sequence of trigeminy, a different arrhythmia class, just by increasing the processing time at the place p3 by 1 sec.

Given a P, R sequence to be modeled, some parameters such as the SA autorhythmic rate and AV conduction delay have direct correspondence to the given data and are thus relatively easy to assign; however, other parameters such as refractory periods cannot be directly observed from the data and must be chosen intelligently. The parameter values listed in Table I are chosen so that the simulation results match the qualitative characteristics of P, R wave sequences for each cardiac arrhythmia.

5. Conclusion

In this paper we have described a systematic procedure for constructing concise mathematical models capable of generating the P, R wave patterns characteristic of different arrhythmias. In particular, there is a straightforward way in which one proceeds from a phenomenological description to a block diagram and then to a stochastic Petri net. The particular aspects of cardiac physiology of importance in modeling any arrhythmia are captured in the structure of the Petri net and in the dynamics of the various elements—as in the dynamics of the AV node portion of our model for Wenckebach in which we model the effect of stage of refractoriness on conduction delay. At a finer level, the detailed timing parameters within the Petri net provide us with the means for modeling the synchronization and control among the cardiac elements and for including the expected level of statistical fluctuation in the observed wave sequence. For example, in a normal wave sequence the SA autorhythmic rate is sufficiently high compared to those of other autorhythmic sites so that the SA node continually resets the other sites and controls the rhythm. Similarly, if the SA rate were sufficiently slow in the Wenckebach model, the Wenckebach phenomenon would not be observable as the AV node would have sufficient time to recover between successive excitations.

In our opinion the modeling approach we have presented offers a useful and flexible framework for modeling cardiac activity at different levels of physiological detail. There are, of course, a variety of directions for further work. First, as pointed out at the end of the preceding section, there is the issue of how to select the timing parameters systematically to realize a desired P, R sequence. The design of an automatic algorithm that estimates these parameters based on a given P, R sequence and a set of physiological constraints (corresponding to particular cardiac rhythms) would be of significant value. The development of hypothesis testing methods for rhythm classification based on Petri net models is another research direction that we feel holds much promise.

Acknowledgments

This research was supported in part by the Air Force Office of Scientific Research under Grant AFOSR-82-0258. In addition, the work of the first author was partially supported by the Harvard–MIT Health Science and Technology Medical Engineering and Medical Physics Fellowship.

REFERENCES

1. GERSCH, W. *et al.* Cardiac arrhythmia classification: A heart-beat interval–Markov chain approach. *Comput. Biomed. Res.* **3,** 385 (1970).
2. GUSTAFSON, D. E., *et al.* ECG/VCG rhythm diagnosis using statistical signal analysis, part I. *IEEE Trans. Biomed. Eng.* **BME-25**(4), 344 (1978).
3. DOERSCHUK, P. C. "A Markov Chain Approach to Electrocardiogram Modeling and Analysis." Ph.D. thesis, Massachusetts Institute of Technology, 1985.
4. PETERSON, J. L. Petri nets. *Comput. Surv.* **9**(3), 223 (1977).
5. PETERSON, J. L. "Petri Net Theory and the Modeling of Systems." Prentice–Hall, Englewood Cliffs, NJ, 1981.
6. MARSON, M. A., *et al.* On Petri nets with stochastic timing. *In* "International Workshop on Timed Petri-Nets 1985," pp. 80–87.
7. RAMAMOORTHY, C. V., AND HO, G. S. Performance evaluation of asynchronous concurrent systems using Petri nets. *IEEE Trans. Software Engi.* **SE-6**(5), 440 (1980).
8. WILEY, R. P. "Performance Analysis of Stochastic Timed Petri Nets." Ph.D. thesis, Massachusetts Institute of Technology, 1986.
9. MOLLOY, M. K. Performance analysis using stochastic Petri nets. *IEEE Trans. Comput.* **C-31**(9), 913 (1982).
10. LEBLANC, A. R., AND ROBERGE, F. A. Present state of arrhythmia analysis by computer. *Canad. Med. Assoc. J.* **108,** 1239 (1973).
11. BONNER, R. E., AND SCHWETMAN, H. D. Computer diagnosis of electrocardiograms. III. A computer program for arrhythmia diagnosis. *Comput. Biomed. Res.* **1,** 387 (1968).
12. WILLEMS, J. L., AND PIPBERGER, H. V. Arrhythmia detection by digital computer. *Comput. Biomed. Res.* **5,** 263 (1972).